JOURNAL OF ANIMAL BEHAVIOUR AND BIOMETEOROLOGY

RESEARCH ARTICLE
Published Online: February 24, 2026
https://doi.org/10.31893/jabb.2026006

Chronic scrotal heat stress induces dose-dependent collapse of male sexual behavior in mice

Phuc Dang-Ngoc[abc] | **Tam Le-Minh**[d] | **Tung Nguyen-Thanh**[a]

[a]Regenerative Medicine Core Research Group, Faculty of Basic Science, University of Medicine and Pharmacy, Hue University, Hue, Vietnam.
[b]Institute of Biotechnology, Hue University, Hue, Vietnam.
[c]Faculty of Medicine, Dong A University, Da Nang, Vietnam.
[d]Department of Obstetrics and Gynecology, Hue University of Medicine and Pharmacy, Hue University, Hue, Vietnam.

Abstract Scrotal hyperthermia is known to impair male reproductive physiology. However its dose- and time-dependent effects on copulatory behaviors have not been fully characterized. This study aimed to systematically quantify the longitudinal effects of chronic scrotal heat stress at moderate (37°C) and severe (40°C) temperatures on the sexual behavior of male mice and correlate these behaviors with testicular mass. Male ICR mice were randomized into control, moderate-heat (H37), and severe-heat (H40) groups. Copulatory behaviors, including mounting, intromission, and ejaculation parameters, were assessed weekly for seven weeks. Testicular and body weights were measured at the conclusion of the study. Control mice maintained stable sexual behavior throughout the study. In the H37 group, progressive impairment was observed starting at week three; with increasing mount, intromission, and ejaculation latencies and decreasing, whereas the frequencies of these behaviors correspondingly decreased over the seven-week period. The H40 group exhibited more severe and rapid deterioration. Behavioral latency increased sharply through week five before all copulatory activities,—including mounting, intromission, and ejaculation,—ceased entirely from week six onward. These behavioral deficits were linked to a significant, dose-dependent reduction in testicular mass. Chronic scrotal heat stress impairs male sexual performance in a dose- and time-dependent manner, ranging from gradual functional decline to complete behavioral collapse. This study established a robust murine model with sensitive behavioral endpoints that is useful for investigating the pathophysiology of heat-induced reproductive dysfunction and for evaluating potential therapeutics.

Keywords: animal, sexual behavior, hyperthermia, scrotum, testis, male reproduction, ICR mice

1. Introduction

Heat stress is one of the most important environmental factors affecting reproductive performance in mammals. Its impact is becoming increasingly significant in the context of global climate change (Hansen, 2009; Khan et al., 2023). In most male mammals, the testes are located outside the body in the scrotum. This anatomical arrangement maintains a testicular temperature approximately 2–8°C lower than the core body temperature, which is essential for normal spermatogenesis (Hamilton et al., 2016; Hansen, 2009). When this thermoregulatory mechanism is disrupted, elevated testicular temperature can result in severe and long-lasting impairments of the reproductive system (Durairajanayagam et al., 2015). Heat stress reduces semen quality, lowers sperm count, impairs motility, and exacerbates morphological abnormalities (Hoang-Thi et al., 2022).

Heat stress affects the testes through complex cellular and molecular mechanisms. Germ cells, especially spermatocytes, are highly temperature-sensitive and undergo apoptosis, which markedly reduces sperm production (Kim et al., 2013; Paul et al., 2009). Heat-induced damage to these cells reduces their supportive capacity and causes endocrine dysregulation (Aldahhan & Stanton, 2021; Nguyen-Thanh et al., 2022). Testicular cells can activate protective pathways, such as ERK1/2 and MK2 kinases, to counteract injury and regulate cell survival and mitigate damage (Cai et al., 2021). Testicular hyperthermia also promotes oxidative stress, which is characterized by an imbalance between reactive oxygen species (ROS) and antioxidant defenses, resulting in damage to lipids, proteins, and DNA (Dutta et al., 2019; Houston et al., 2018). Heat stress can also disrupt the blood–testis barrier (BTB), compromising the specialized microenvironment needed for normal spermatogenesis (Zhao et al., 2024).

Sexual behavior is controlled by gonadal hormones and regulated by the hypothalamic–pituitary–gonadal (HPG) axis. This axis interacts with the hypothalamic–pituitary–adrenal (HPA) axis and is sensitive to stressors, which can impair reproductive function (Plant, 2015; Phumsatitpong et al., 2021). Therefore, understanding the impact of heat stress on sexual behavior requires consideration of both local testicular effects and potential alterations at the central neuroendocrine level.

Acute heat stress models, such as exertional heat stroke (EHS), have been shown to cause erectile dysfunction and testicular damage (Lin et al., 2021). However, such studies primarily reflect the immediate effects of a single severe stress event

 Received: October 1, 2025 | Accepted: February 7, 2026

and do not account for the cumulative effects of chronic heat stress exposure. However, a critical knowledge gap exists in understanding how this physiological damage progressively translates into quantifiable behavioral deficits, as there is a lack of systematic, longitudinal data detailing how chronic heat stress of varying intensities alters the complete repertoire of male copulatory behavior over time.

Therefore, the objective of this study was to quantitatively and systematically evaluate the effects of chronic scrotal heat stress on the sexual behavior of male mice. By applying two different temperatures (37°C and 40°C) to simulate moderate and severe levels of stress, this study not only assessed changes in behavioral indices over time but also correlated these changes with physiological parameters, such as body weight and testicular mass. This integrative approach is expected to address current knowledge gaps and provide a more comprehensive understanding of the relationship between physiological injury and heat stress–induced impaired sexual behavior.

2. Materials and Methods

2.1. Animals and ethical approval

Male ICR mice (8 weeks old, 30–35 g) were obtained from the National Institute for Control of Vaccines and Biologicals (NICVB), Vietnam. The animals were housed under standard laboratory conditions (25 ± 1°C, 12 h light/dark cycle) with ad libitum access to food and water and acclimated for 7 days prior to experimentation (Feige-Diller et al., 2020).

Fifteen male mice were randomly assigned to three groups (n = 5/group): a control group (CON, 25°C), a moderate heat stress group (H37, 37°C), and a severe heat stress group (H40, 40°C) (Nguyen-Thanh et al., 2022).

2.2. Chronic scrotal heat stress protocol

The experimental timeline spanned seven weeks divided into a two-week pre-treatment phase (D0 to week 2) and a five-week chronic heat stress application period (week 2 to week 7). Mice in the H37 and H40 groups underwent chronic scrotal heat stress for five consecutive weeks (week 2 to week 7). The protocol involved immersing the lower body of the mice in a temperature-controlled water bath for 10 minutes, twice daily with a 10-minute interval, for six days a week. This protocol was adapted from our previous study. The control mice were handled similarly but with water immersion at room temperature (25°C) (Nguyen-Thanh et al., 2022).

2.3. Preparation of stimulus females

The mice were first administered meloxicam subcutaneously at a dose of 5 mg/kg for analgesia. Anesthesia was induced by the intraperitoneal injection of a mixture of ketamine (50 mg/kg) and xylazine (5 mg/kg) prepared in sterile water (Luengo-Mateos et al., 2024). The depth of anesthesia was confirmed by the absence of voluntary movements for at least 30 s, stable respiration (approximately one breath every 2 s or slower), and loss of the pedal reflex upon gentle paw pinch. Ophthalmic ointment (Puralube) was applied to the eyes to prevent corneal dryness (Liu et al., 2020).

The abdominal surgical area was shaved with a hair trimmer and disinfected with 2% chlorhexidine (Luengo-Mateos et al., 2024). Once adequate anesthesia was achieved, the mice were placed in the supine position and secured to the surgical table with adhesive tape.

2.4. Ovariectomy

Bilateral ovariectomy was performed using a standardized microsurgical protocol (Figure 1). A midline abdominal incision (~0.5 cm) was made in the disinfected area using a microsurgical scalpel, which was cut through the skin, subcutaneous fat, and muscle (Rhodes, 2017). The right and left ovaries, which were surrounded by white adipose tissue and attached to the uterus, were gently exteriorized via forceps. The ovaries were excised via an electrosurgical scalpel, and approximately 1.0 cm of tissue was removed. The oviducts were examined to confirm the complete removal of the ovarian tissue. The uterine horns were then repositioned into the abdominal cavity, and the muscle and skin layers were closed with absorbable sutures to prevent herniation or other complications. The surgical site was disinfected with 2% chlorhexidine digluconate solution.

Fifteen female mice were used for ovariectomy to prepare them for sexual behavior testing. After surgery, the animals were monitored daily for signs of infection, poor wound healing, or abnormal behavior. Mice that experienced postoperative complications or failed to recover within 72 hours were excluded from subsequent behavioral experiments.

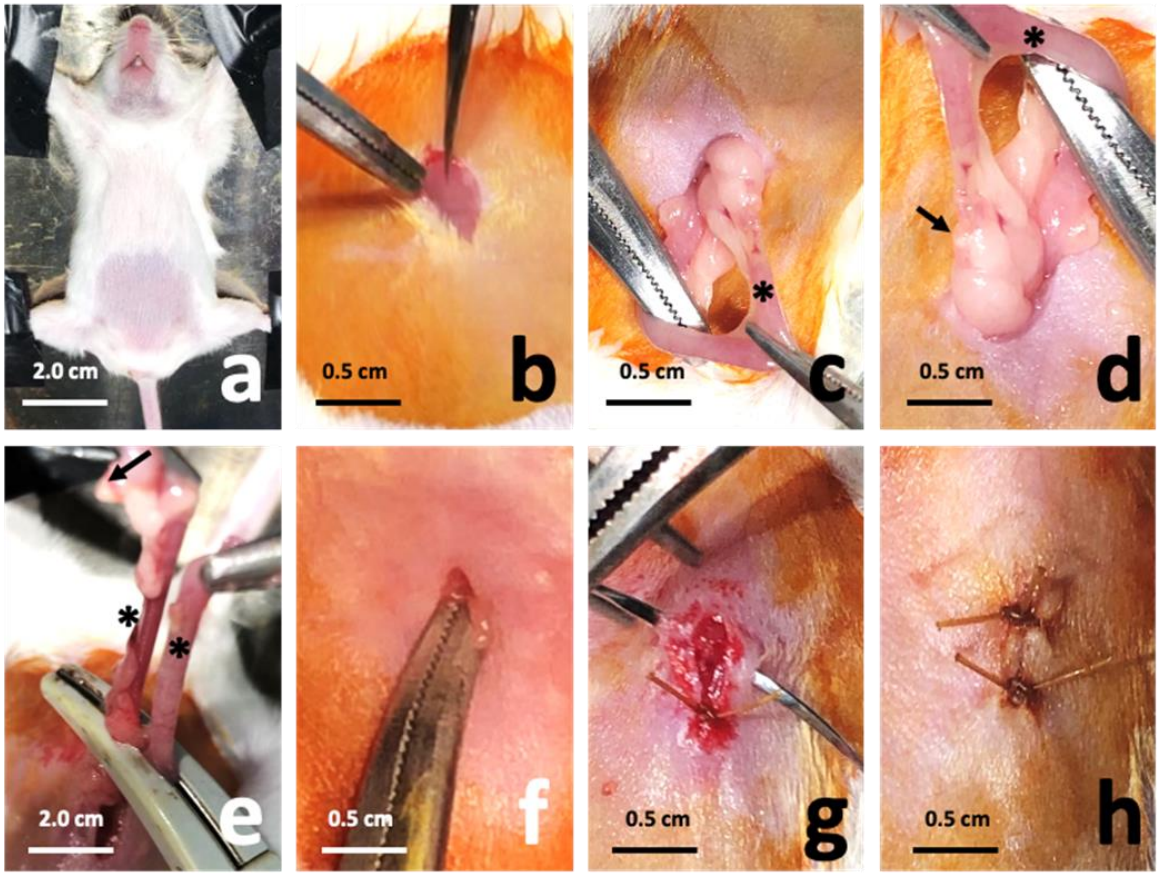

Figure 1 Step-by-step surgical procedure for bilateral ovariectomy in mice.

(a) The anesthetized mouse is positioned in dorsal recumbency, and the surgical site is shaved. (b) Following disinfection, a midline abdominal incision (~0.5 cm) was made through the skin and peritoneum. (c) The uterine horn and ovary are gently exteriorized via forceps. (d) The periovarian fat pad is dissected to clearly identify the ovary. (e) The ovary is excised via an electrosurgical scalpel. (f) The uterine horn is repositioned into the abdominal cavity. (g) The muscle and skin layers were closed with absorbable sutures. (h) The wound is disinfected postsurgically. The arrow indicates the ovary; the asterisk indicates the uterine horn.

2.5. Postoperative care

Only animals that recovered without postoperative complications were included in the postoperative care and subsequent behavioral experiments. Postoperative care is essential to ensure the recovery of experimental animals. Following surgery, female mice were administered intraperitoneal penicillin sodium (10,000 units/10 g body weight) for infection prophylaxis and subcutaneous buprenorphine for pain relief (Liu et al., 2020). To prevent dehydration, a pre-warmed (37°C) 0.9% saline solution was injected subcutaneously (Luengo-Mateos et al., 2024).

Each mouse was placed in a separate sterile cage in a well-ventilated area and closely monitored for 1–2 h until full recovery from anesthesia. During this period, the mice were kept on clean paper towels in cages without bedding material. The animals were subsequently maintained for 14 days with ad libitum access to food and water before being used in further experiments (Luengo-Mateos et al., 2024).

The estrous stage in female mice was determined via vaginal smear cytology. The absence of estrous cycle changes confirmed the success of ovariectomy (Luengo-Mateos et al., 2024).

2.6. Artificial induction of estrus in female mice

The timeline of ovariectomy, postoperative recovery, hormonal induction of estrus, and subsequent pairing for the assessment of male sexual behavior is illustrated in Figure 2. Following bilateral ovariectomy, female mice were allowed a 2-week recovery period before the experiment. To induce estrus, each mouse received a subcutaneous injection of 10 μg estradiol benzoate 48 h before pairing with a male mouse, followed by an additional injection of 5 μg estradiol benzoate 24 h prior to pairing. Subsequently, 500 μg of progesterone was administered subcutaneously 4–7 h before pairing (Ogawa et al., 2000).

After the hormonal regimen was completed, females were introduced to males to assess their sexual behavior. Estrus was confirmed when the female exhibited sexual receptivity, defined as accepting at least three intromissions from a sexually active and experienced male during cohabitation in the same cage.

2.7. Preparation for sexual behavior testing

Sexual behavior testing of male mice was performed in an open rectangular arena (40 cm × 30 cm × 25 cm; length × width × height) (Liu et al., 2020). The arena walls were constructed of black Plexiglass, except for the transparent front wall, which allowed direct observation. To maintain standardized conditions, all experiments were conducted during the early hours of the dark phase of the light/dark cycle, when male mice display peak sexual activity. During behavioral testing, the room was illuminated with dim red light (<20 lx) to mimic dark-phase conditions while still permitting accurate video recording. A higher light intensity (approximately 650 lx) was used only briefly during animal handling and arena preparation and was switched off before the start of the behavioral sessions. Direct light exposure to the animals was strictly avoided to prevent abnormal behavioral responses (Liu et al., 2020).

Before the stimulus female was introduced, each male mouse was allowed a 5-min habituation period in the arena to minimize stress and ensure consistent baseline exploratory behavior. Following habituation, the stimulus female was placed in the arena, and sexual behavior was recorded continuously via a digital video camera equipped with a memory card for subsequent offline analysis.

2.8. Acclimatization of the mice prior to sexual behavior assessment

The laboratory environment was kept quiet and free from distractions. The mice were placed individually in the testing cage and allowed to explore the environment freely for 30 min. This acclimatization procedure was conducted on two consecutive days prior to the experimental session to minimize stress associated with exposure to a new environment (Liu et al., 2020).

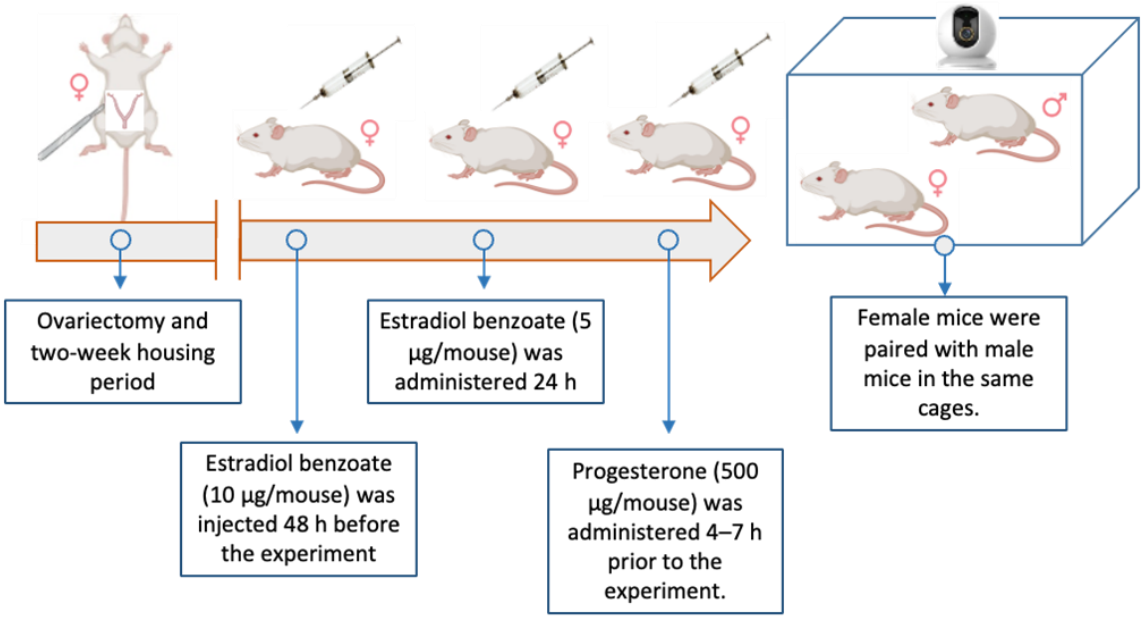

Figure 2 Timeline of ovariectomy, hormonal induction of estrus, and pairing for the assessment of male sexual behavior.

The protocol began with bilateral ovariectomy, after which the female mice were housed for a two-week recovery period. To artificially induce estrus, a sequential hormonal regimen was administered subcutaneously. Females first received estradiol benzoate (10 µg/mouse) 48 hours before the planned behavioral test, followed by a second dose of estradiol benzoate (5 µg/mouse) 24 hours prior to the test. Finally, to maximize sexual receptivity, progesterone (500 µg/mouse) was administered 4–7 hours before pairing. Once hormonally primed, the stimulus females were placed with male mice for video-recorded behavioral assessment.

2.9. Behavioral data extraction

The parameters used to assess male sexual behavior are shown in Figure 3. Video recordings of copulatory behavior were analyzed to quantify male sexual activity. The following parameters were assessed according to Liu et al. (2020): mount latency (ML), defined as the time from the introduction of the stimulus female to the first mounting attempt (s); mount frequency (MF), the total number of mounts observed within a 30-min testing period; intromission latency (IL), the time from

pairing to the first vaginal intromission (s); intromission frequency (IF), the total number of vaginal intromissions within 30 min; ejaculation latency (EL), the time from the first intromission to the first ejaculation (s); and postejaculatory interval (PEI), the time from the first ejaculation to the subsequent mounting or intromission that initiated a new copulatory series (s) (Liu et al., 2020).

Diagrammatic representation of the quantitative parameters used to assess the male mouse copulatory sequence over a 30-minute observation period. The initial phase was characterized by key parameters: mount latency (ML), measured as the time from the introduction of the female (pairing) to the first mount, and intrusion latency (IL), the time from pairing to the first successful intromission. The frequency of these behaviors, the mount frequency (MF) and the intromission frequency (IF), represents the total number of mounts and intromissions, respectively. The consummatory phase was assessed by ejaculation latency (EL), defined as the time from the first intromission to the first ejaculation. Finally, the recovery period was measured by the post-ejaculatory interval (PEI), the time from the first ejaculation to the subsequent mounting event.

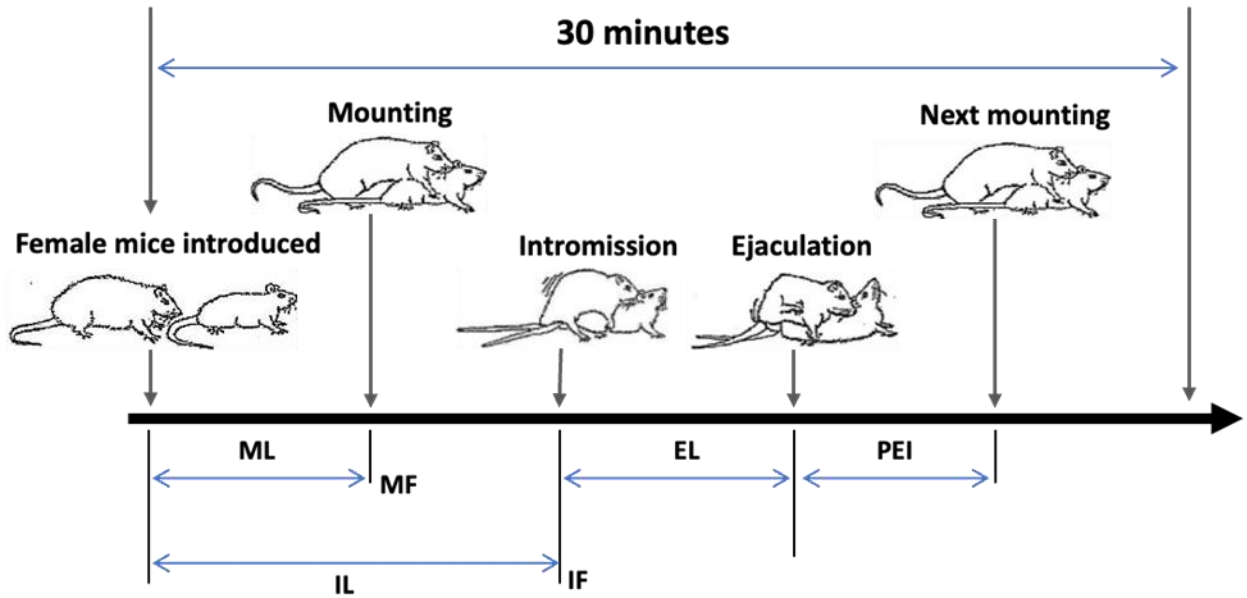

Figure 3 Diagram illustrating the parameters used to assess male mouse sexual behavior .

2.10. Statistical analysis

The data were analyzed via IBM SPSS Statistics (version 18).

The longitudinal data were analyzed using Two-way repeated-measures ANOVA, followed by Bonferroni post hoc correction, was used to assess the effects of group and time. The model included group (CON, H37, H40) as the between-subject factor and time (D0 through 7W) as the within-subject factor, with the primary interest being the group × time interaction. The data are presented as the means ± SDs, with statistical significance set at $p < 0.05$.

3. Results

3.1. Effects of heat stress on body weight and testicular mass in male mice

3.1.1. Chronic heat stress induces a dose-dependent reduction in body weight

The longitudinal effects of chronic scrotal heat stress on the body weights of male mice are presented in Table 1 and visualized in Figure 4a. At baseline (D0), there was no significant difference in body weight among the three groups: 34.60 ± 0.89 g in the control (CON) group, 35.80 ± 1.64 g in the moderate-heat (H37) group, and 35.00 ± 0.71 g in the severe-heat (H40) group.

Table 1 Effects of heat stress on the body weights of male mice over time.

Week Group	D0	1 W	2 W	3 W	4 W	5 W	6 W	7 W
CON	34.60 ± 0.89	35.60 ± 1.34	36.80 ± 1.30	37.40 ± 0.89	38.00 ± 0.71	38.80 ± 0.84	39.00 ± 0.71	39.60 ± 0.89
H37	35.80 ± 1.64	35.80 ± 1.64	35.20 ± 0.84	34.20 ± 0.84	33.60 ± 0.55	33.40 ± 0.55	32.80 ± 0.45	31.80 ± 0.84
H40	35.00 ± 0.71	34.40 ± 0.55	33.60 ± 0.55	32.80 ± 0.45	32.20 ± 0.45	31.00 ± 0.00	30.60 ± 0.55	30.20 ± 0.45

Over the 7-week period, the mice in the control group exhibited a consistent and healthy increase in body weight, increasing to 39.60 ± 0.89 g by week 7. This steady growth is clearly illustrated by the upward sloping line for the CON group in Figure 4a, representing normal development under standard conditions.

In contrast, both heat-stressed groups experienced significant weight loss. The H37 group maintained its weight for the first two weeks before showing a progressive decline, starting at week 3 (34.20 ± 0.84 g) and ending at 31.80 ± 0.84 g at week 7. The H40 group displayed a more immediate and severe reduction, with body weight decreasing steadily throughout the experiment to a final value of 30.20 ± 0.45 g. These downward trends are visually confirmed in Figure 4a, where the slope of the line for the H40 group was steeper than that of the H37 group, indicating more severe weight loss. Overall, the results show that heat stress causes a dose- and time-dependent reduction in body weight.

3.1.2. Heat stress causes significant, dose-dependent testicular atrophy

Chronic scrotal heat stress induced a significant reduction in testicular mass, as detailed in Table 2 and Figure 4c-d. The mean absolute testicular weight of the control (CON) group at the end of the study was 0.19 ± 0.03 g. In contrast, the weights were substantially lower in the moderate-heat (H37) group (0.11 ± 0.01 g) and the severe-heat (H40) group (0.09 ± 0.02 g). The statistical analysis presented in Figure 4c confirms that, compared with that of the control group, the reduction in testicular weight was highly significant for both the H37 group ($P < 0.05$) and the H40 group ($P < 0.05$).

Table 2 Physiological parameters of male mice after seven weeks of exposure to chronic scrotal heat stress.

Group	Body weight (g)		Testicular weight (g)		Testis-to-body weight ratio (%)	
	Mean	SD	Mean	SD	Mean	SD
CON	39.60	0.89	0.19	0.03	0.48	0.08
H37	31.80	0.84	0.11	0.01	0.34	0.03
H40	30.20	0.45	0.09	0.02	0.30	0.07

This pattern of atrophy was also evident in the relative testis-to-body weight ratio. The ratio for the CON group was 0.48 ± 0.08%. As shown in Figure 4d, this value was significantly greater than the ratios observed in both the H37 group (0.34 ± 0.03%; $P < 0.05$) and the H40 group (0.30 ± 0.07%; $P < 0.05$). Collectively, these data demonstrate clear, dose-dependent testicular atrophy in response to the increasing intensity of chronic heat stress.

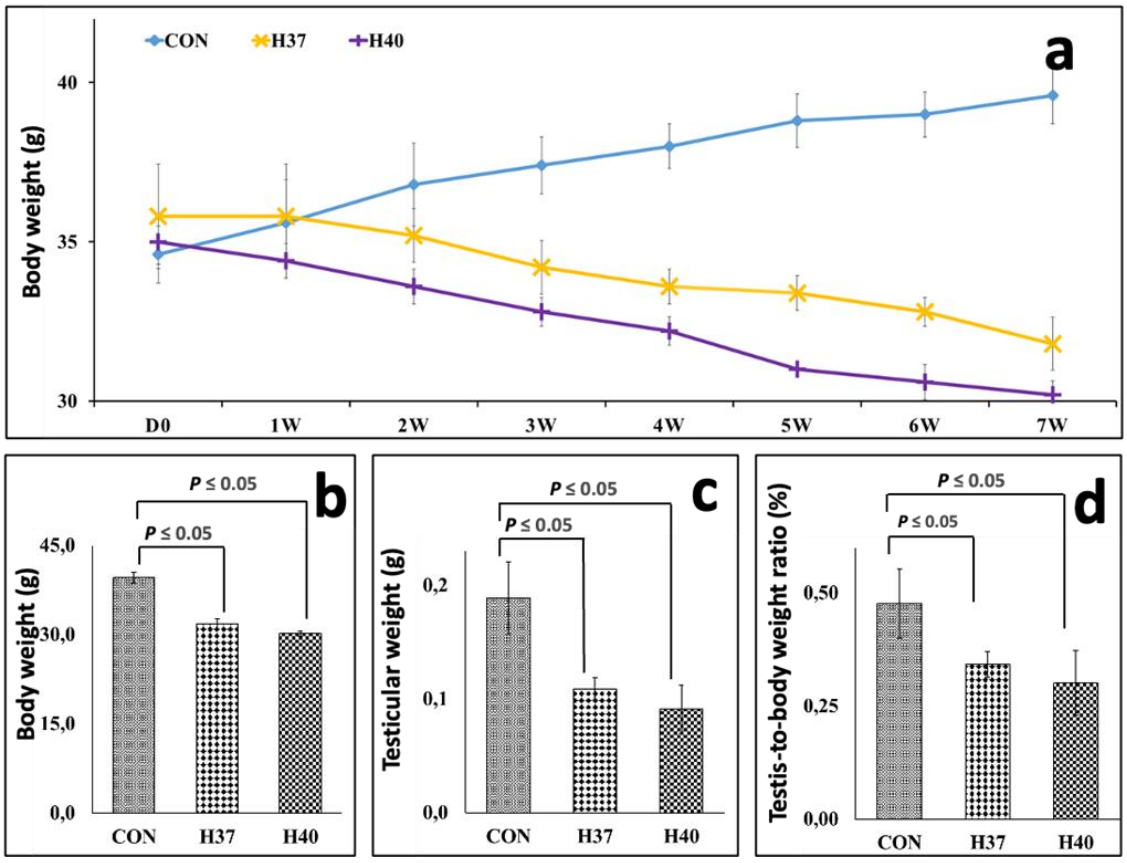

Figure 4 Chronic heat stress induces dose-dependent reductions in body weight and testicular mass.

(a) The panel displays the longitudinal changes in body weight over the seven-week experimental period. (b) Terminal body weight at week 7. (c) Terminal testicular weight at week 7. (d) The relative testis-to-body weight ratio at week 7

3.2. Effects of heat stress on sexual behavior

3.2.1. Qualitative assessment of male copulatory behavior

The male mouse copulatory sequence consists of a stereotyped series of behaviors, as illustrated in Figure 5. The sequence is initiated with investigatory actions, where the male approaches the female and engages in anogenital sniffing. This is followed by the copulatory phase, which includes the first mounting and successful vaginal intromission. Between intromissive events, the male typically performs a brief bout of genital grooming before proceeding to subsequent intromission. The sequence culminates in the consummatory act of ejaculation, identified by a characteristic posture, which is followed by a longer period of postejaculatory genital grooming.

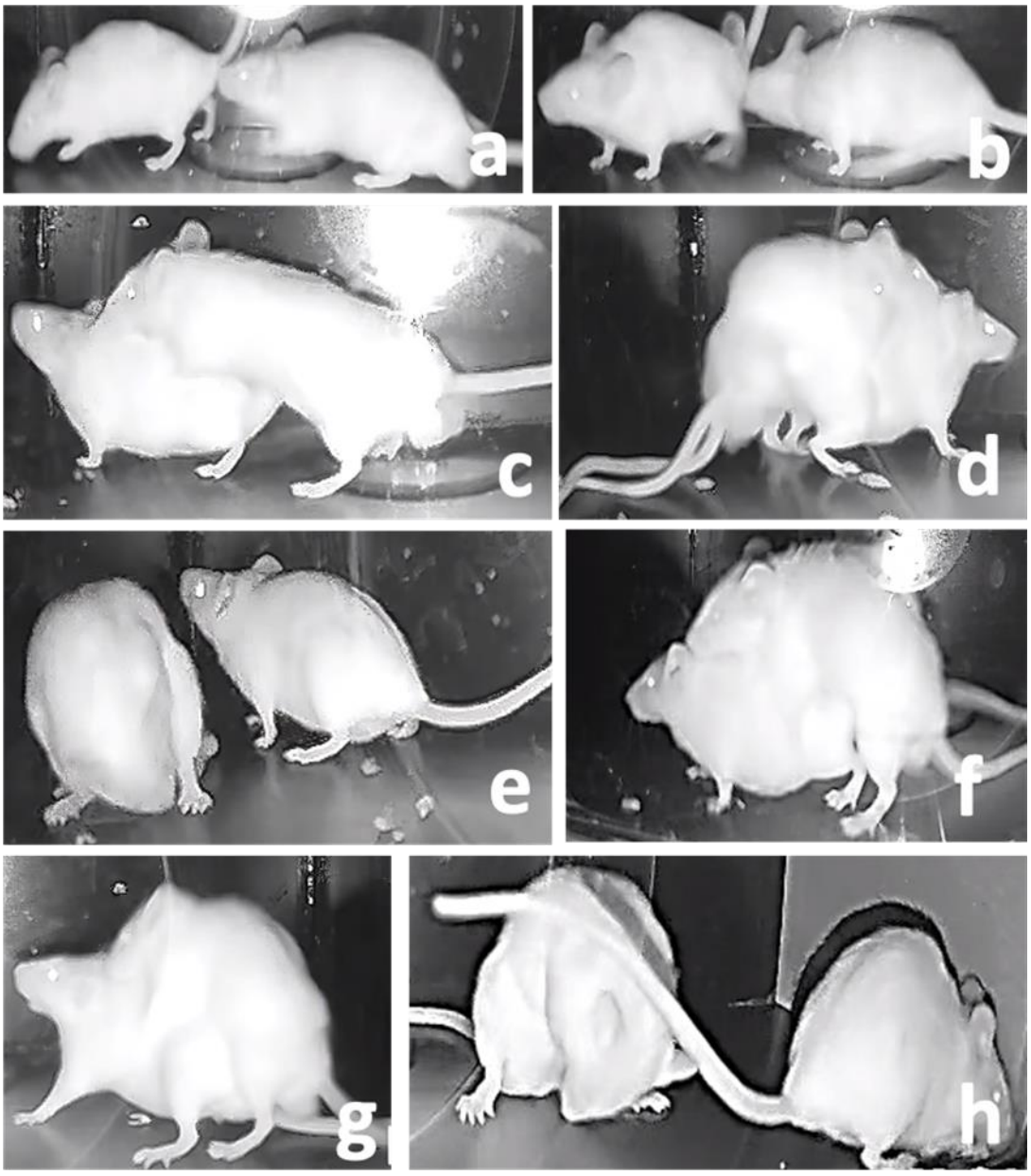

Figure 5 Representative images of key events in the male mouse copulatory sequence.

Representative images of the key events that constitute the male mouse copulatory sequence. The sequence begins with initiating behaviors, including the male approaching the female (a) and conducting anogenital investigations (b). This is followed by the first mount (c) and successful vaginal intromission (d). Between intromissive events, the male typically engages in a brief period of genital grooming (e) before proceeding to a subsequent intromission (f). The copulatory series culminates

in ejaculation, characterized by a distinct posture (g), which is followed by a longer bout of postejaculatory genital grooming (h).

3.2.2. Effects of heat stress on copulatory initiation: mounting latency and frequency

Chronic scrotal heat stress induced significant, dose- and time-dependent impairments in mounting behavior (Figure 6a, 6b). In the control group, the mounting latency (ML) remained stable throughout the 7-week observation period, ranging from 377.60 ± 31.15 s (week 3) to 434.40 ± 37.69 s (D0). The mounting frequency (MF) was also consistent, recorded at 3.20 ± 0.84 at baseline and 4.00 ± 0.71 at week 7, establishing a stable physiological baseline for comparison (Table 3).

In contrast, the moderate-heat (H37) group exhibited a progressive deterioration in mounting behavior. As depicted in Figure 6a, the ML began to increase notably at week 3 (484.80 ± 39.26 s) and rose steadily, reaching its peak at week 7 (759.60 ± 34.68 s). Concurrently, MF declined in parallel, dropping from 2.40 ± 0.55 at week 3 to 1.00 ± 0.00 by week 7 (Figure 6b, Table 3). This pattern demonstrated that moderate heat stress significantly delayed the initiation of copulatory behavior and reduced its frequency.

The severe heat (H40) group displayed more rapid and profound impairment. ML increased sharply from week 3 (718.60 ± 52.36 s) and peaked at 917.80 ± 19.19 s in week 5. Critically, mounting behavior was subsequently and completely abolished; consequently, both the ML and MF values for the H40 group were recorded as non-occurrence at weeks 6 and 7 (Table 3). These results demonstrate that prolonged exposure to high-intensity heat stress culminates in a total elimination of mounting behavior, clearly visualized as a behavioral collapse (Figure 6)

3.2.3. Effects of heat stress on intromission behavior: intromission latency and frequency

Chronic heat stress resulted in a dose- and time-dependent failure of intromission behavior (Figure 6c, 6d). Intromission behavior in the control group was maintained within the normal physiological range throughout the experiment. The remission latency (IL) was stable and recorded at 615.00 ± 13.42 s at baseline (D0) and 564.40 ± 59.54 s at week 7. The IF showed a slight upward trend, increasing from 6.60 ± 0.55 to 7.40 ± 0.55 over the same period, establishing a consistent baseline for performance (Table 3).

In the moderate-heat (H37) group, progressive impairment was observed. As shown in Figure 6c, the IL began to increase significantly at week 3 (756.00 ± 44.70 s) and continued to rise, reaching 966.60 ± 28.09 s by week 7. Moreover, the IF decreased steadily, from 4.60 ± 0.55 at week 3 to 2.20 ± 0.45 at week 7, which represented only approximately one-third of the control value (Figure 6d, Table 3).

The severe heat (H40) group presented the most severe impairments, leading to a complete loss of intromission. The ILs increased sharply from week 3 (915.00 ± 29.52 s), peaked at 988.60 ± 10.97 s at week 5. In parallel, the IF also declined drastically, decreasing to 3.20 ± 0.84 at week 3 and 2.00 at week 5. Subsequently, intromission behavior was completely abolished, resulting in both IL and IF being recorded as Non-occurrence from Week 6 onward (Table 3). This complete behavioral cessation is clearly visualized as a collapse in Figure 6.

3.2.4. Effects of heat stress on ejaculatory function and recovery: ejaculation latency and post-ejaculatory interval

The consummatory phases of sexual behavior, ejaculation and subsequent recovery were significantly impaired by chronic heat stress in a dose- and time-dependent manner (Figure 6e, 6f).

In the control group, the ejaculation latency (EL) remained stable after an initial decline, ranging between 142.60 ± 13.77 s and 161.40 ± 6.80 s from week 2 to week 7. The postejaculatory interval (PEI) in this group gradually decreased from 205.80 ± 17.12 s at baseline to 153.40 ± 30.23 s at week 7, reflecting a consistent baseline for comparison (Table 3).

Exposure to moderate heat (H37) induced a persistent increase in both parameters. As shown in Figure 6e, EL increased steadily from 200.20 ± 16.50 s on D0 to its highest level at week 7 (381.20 ± 57.95 s). Similarly, the PEI increased from 219.20 ± 16.69 s on D0 to 322.60 ± 42.26 s on week 7, suggesting that moderate heat stress not only delayed ejaculation but also extended the recovery period before the resumption of mating activity (Figure 6f, Table 3).

The severe heat (H40) group presented the most profound changes, culminating in a complete loss of ejaculatory function. EL increased to a peak of 384.40 ± 19.68 s at week 5, after which the males no longer ejaculated. Correspondingly, the PEI increased to 375.60 ± 33.97 s at week 5, followed by a complete loss of measurable values from week 6, reflecting a total collapse of copulatory function (Table 3).

(a) Mounting latency (ML); (b) Mounting frequency (MF); (c) Intromission latency (IL); (d) Intromission frequency (IF); (e) Ejaculation latency (EL); (f) Postejaculatory interval (PEI)

4. Discussion

This study systematically investigated the impact of chronic scrotal heat stress on male sexual behavior in mice by monitoring a comprehensive set of behavioral indices, including mount latency and frequency (ML–MF), intromission latency and frequency (IL–IF), and ejaculation latency and postejaculatory interval (EL–PEI). The results revealed distinct temperature-

and time-dependent effects. While control animals maintained stable performance throughout the experimental period, exposure to 37°C progressively delayed copulatory initiation, reduced behavioral frequency, and prolonged recovery intervals. More strikingly, exposure to 40°C resulted in rapid deterioration of sexual activity and complete collapse of mounting, intromission, and ejaculation behaviors after five weeks. The decline in sexual behavior, particularly the complete collapse in the H40 group, is likely multifactorial, stemming from both direct reproductive impairment (testicular atrophy) and generalized physiological debilitation. These findings establish a reliable animal model in which behavioral alterations accurately reflect the physiological consequences of testicular hyperthermia.

Table 3 Quantitative analysis of sexual behavior parameters in male mice following chronic scrotal heat stress.

Parameter	Week Group	D0	1 W	2 W	3 W	4 W	5 W	6 W	7 W
ML (s)	CON	434.40	421.60	386.00	377.60	404.20	411.40	384.60	399.20
		± 37.69	± 22.78	± 15.17	± 31.15	± 17.80	± 32.36	± 24.03	± 52.97
	H37	397.60	395.80	377.80	484.80	590.60	649.80	700.80	759.60
		± 20.18	± 32.90	± 25.84	± 39.26	± 50.10	± 49.44	± 40.11	± 34.68
	H40	428.40	416.00	410.20	718.60	838.80	917.80	Non-occurrence	Non-occurrence
		± 26.26	± 16.42	± 15.61	± 52.36	± 76.09	± 19.19		
MF	CON	3.20	3.20	3.40	3.60	3.60	3.20	3.80	4.00
		± 0.84	± 0.45	± 0.55	± 0.55	± 0.89	± 1.10	± 0.45	± 0.71
	H37	3.00	3.20	3.60	2.40	2.20	2.00	1.60	1.00
		± 0.00	± 0.45	± 0.55	± 0.55	± 0.45	± 0.00	± 0.55	± 0.00
	H40	2.80	3.60	3.60	1.80	1.20	1.20	Non-occurrence	Non-occurrence
		± 0.45	± 0.55	± 0.55	± 0.45	± 0.45	± 0.45		
IL (s)	CON	615.00	606.00	576.00	568.00	590.40	566.20	560.20	564.40
		± 13.42	± 30.42	± 64.53	± 54.17	± 63.79	± 27.15	± 35.88	± 59.54
	H37	625.00	617.60	620.00	756.00	785.40	849.40	923.80	966.60
		± 10.30	± 12.32	± 82.88	± 44.70	± 48.09	± 93.20	± 61.74	± 28.09
	H40	560.20	577.20	564.80	915.00	976.20	988.60	Non-occurrence	Non-occurrence
		± 32.90	± 115.37	± 122.79	± 29.52	± 20.77	± 10.97		
IF	CON	6.60	6.60	6.40	6.60	6.80	6.40	7.00	7.40
		± 0.55	± 0.55	± 0.55	± 0.55	± 0.84	± 0.55	± 0.71	± 0.55
	H37	5.40	5.60	6.20	4.60	3.80	3.40	2.80	2.20
		± 0.55	± 0.89	± 0.84	± 0.55	± 0.45	± 0.55	± 0.84	± 0.45
	H40	6.20	6.40	7.20	3.20	2.00	2.00	Non-occurrence	Non-occurrence
		± 0.45	± 0.55	± 0.45	± 0.84	± 0.00	± 0.00		
EL(s)	CON	202.60	165.80	149.00	161.40	150.40	142.60	145.80	154.40
		± 15.92	± 13.39	± 5.29	± 6.8	± 5.80	± 13.77	± 19.33	± 20.22
	H37	200.20	196.40	191.60	281.40	340.40	359.20	359.80	381.20
		± 16.50	± 25.37	± 26.77	± 31.57	± 28.83	± 36.38	± 47.41	± 57.95
	H40	208.60	185.60	166.40	306.20	345.40	384.40	Non-occurrence	Non-occurrence
		± 16.79	± 25.37	± 19.33	± 30.82	± 19.71	± 19.68		
PEI (s)	CON	205.80	176.60	160.60	148.00	156.00	171.60	160.00	153.40
		± 17.12	± 21.49	± 17.39	± 22.44	± 23.07	± 30.62	± 19.95	± 30.23
	H37	219.20	222.00	252.80	260.00	300.20	318.80	310.20	322.60
		± 16.69	± 20.09	± 33.63	± 31.28	± 72.66	± 59.44	± 60.25	± 42.26
	H40	218.00	275.40	284.20	335.00	353.80	375.60	Non-occurrence	Non-occurrence
		± 4.64	± 14.60	± 29.00	± 35.80	± 39.02	± 33.97		

The progressive increase in ML and IL, coupled with the concomitant decline in MF and IF, demonstrates that chronic hyperthermia compromises both the initiation and efficiency of copulatory behaviors. Similarly, the prolongation of EL and PEI in the 37°C group indicated delayed consumption and recovery, whereas their disappearance in the 40°C group reflected a total loss of ejaculatory capacity. This concordance across behavioral parameters supports the concept that the entire mating sequence, from initiation to completion, is vulnerable to disruption by heat stress. These observations are consistent with previous findings showing that testicular heat stress impairs spermatogenesis, reduces sperm function, and diminishes overall reproductive capacity (Durairajanayagam et al., 2015; Hansen, 2009).

At the cellular and molecular levels, multiple mechanisms converge to explain these results. Even a single transient exposure to elevated scrotal temperatures induces hypoxia, oxidative stress, and germ-apoptosis, particularly in pachytene spermatocytes and round spermatids (Paul et al., 2009). Under chronic conditions, histopathological studies have documented interstitial inflammation, fibroblast proliferation, and fibrosis in the testes, which collectively impair spermatogenesis and endocrine support (Nguyen-Thanh et al., 2022). These pathologies align with our behavioral findings, where moderate heat stress produced measurable but incomplete behavioral impairment, whereas severe stress led to a threshold-like collapse in reproductive performance.

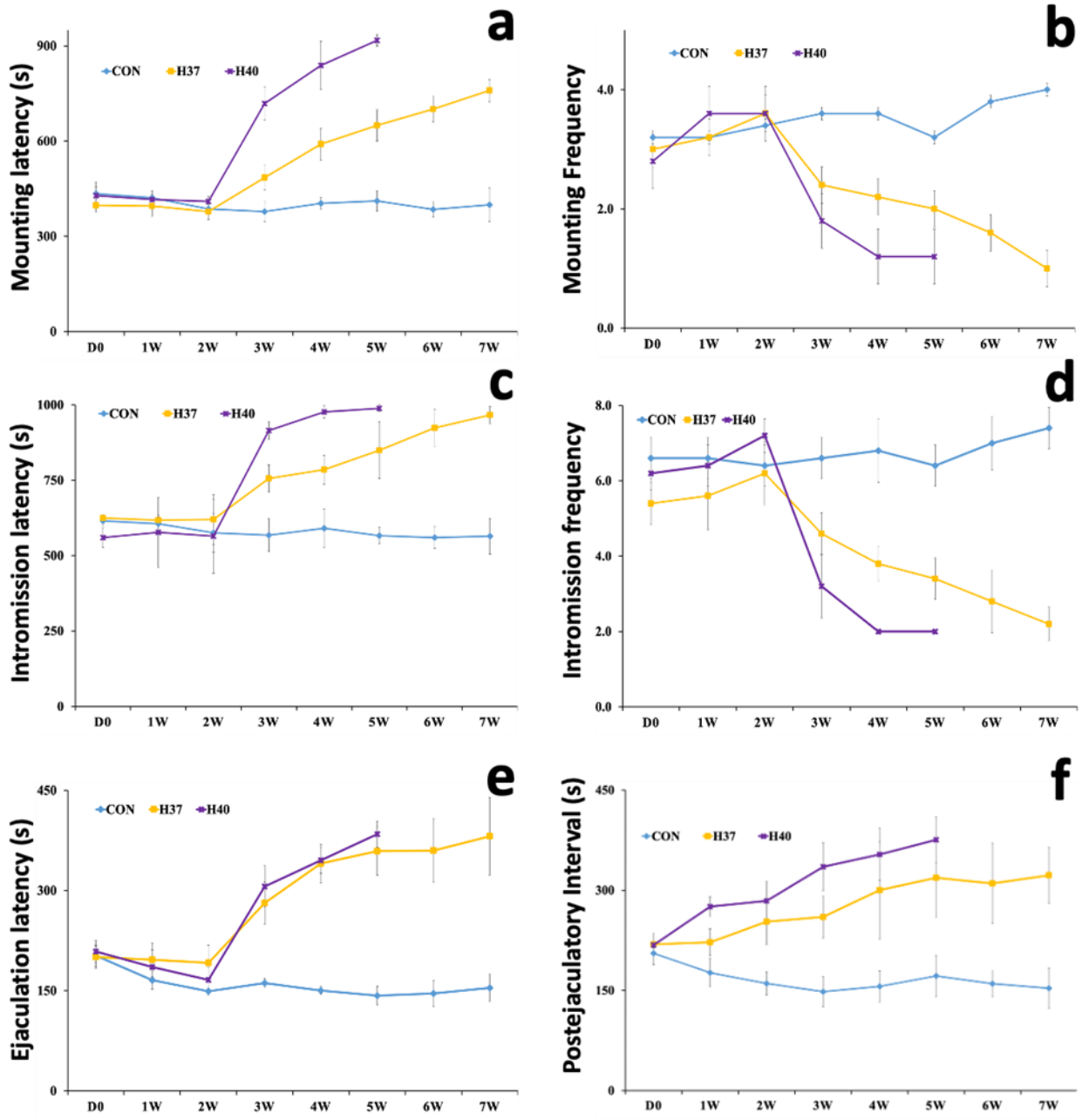

Figure 6 Chronic heat stress progressively impairs sexual behavior in male mice.

Somatic cell dysfunction also plays a critical role in this process. Heat stress disrupts Sertoli cell tight junctions and compromises the blood–testis barrier (BTB), thereby altering the microenvironment required for normal spermatogenesis. Protective interventions, such as melatonin supplementation, have been shown to stabilize BTB integrity and maintain germ cell development (Zhang et al., 2020). In parallel, Leydig cells undergo endoplasmic reticulum stress and apoptosis when exposed to elevated temperatures, leading to reduced testosterone secretion; however, zinc supplementation has been reported to mitigate these effects (Xiong et al., 2022). These findings provide a mechanistic explanation for how somatic cell injury contributes to diminished sexual motivation and copulatory efficiency under hyperthermic conditions.

The neuroendocrine system further amplifies these effects. Sexual behavior is primarily regulated by the hypothalamic–pituitary–gonadal (HPG) axis, which is highly sensitive to stressors through its interaction with the hypothalamic–pituitary–adrenal (HPA) axis. Heat stress disrupts GnRH and LH secretion, alters testosterone dynamics, and reduces male sexual drive (Plant, 2015; Phumsatitpong et al., 2021). Our behavioral data, specifically the progressive increase in latency followed by total behavioral collapse in the 40°C group, are consistent with this integrative model of peripheral testicular injury and central neuroendocrine dysregulation.

The dose–duration dependency observed in this study aligns with previous reviews, indicating that higher intensities and longer heat exposure cause more severe reproductive impairment, with maximal effects typically emerging within 4–5 weeks (Robinson et al., 2023). The complete disappearance of mounting, intromission, and ejaculation in the H40 group after week 5 strongly supports this hypothesis. Similar associations have been reported in humans, where occupations or activities that increase scrotal temperature, such as professional driving, industrial work, or sauna use, are linked to reduced semen quality and increased sperm DNA fragmentation (Durairajanayagam et al., 2015; Zhang et al., 2015).

Several protective strategies have been proposed for this purpose. Antioxidants, such as melatonin and resveratrol, attenuate oxidative stress, suppress apoptosis, and preserve spermatogenesis under hyperthermic conditions (Hafez et al., 2025; Zhang et al., 2020). Zinc supplementation protects Leydig cells from ER stress-induced apoptosis (Xiong et al., 2022), whereas phytochemicals, such as *Curculigo orchioides* extracts, mitigate spermatogenic disruption in murine models (Bui-Le et al., 2023). Together, these findings highlight that a combined approach involving antioxidants, antiapoptotic, and anti-inflammatory agents may offer translational benefits in managing heat-induced reproductive dysfunction.

A limitation of this study is its focus on macroscopic copulatory behaviors without concurrent assessment of underlying biological mechanisms. Specifically, we did not directly assess testosterone levels or measure histopathological or molecular markers, such as oxidative stress and apoptosis, which would clarify the relative contributions of testicular and neuroendocrine mechanisms to the observed functional decline. Furthermore, the relatively small sample size (n=5 per group) limits the statistical power to detect subtle effects and increases the sensitivity of the data to individual outliers. The significant, dose-dependent body weight loss in the heat-stressed groups suggests that systemic physiological stress, beyond specific testicular damage, may have also contributed to the behavioral deficits. Finally, the reversibility of these heat-induced impairments remains unclear, highlighting the necessity for future longitudinal studies to address recovery periods and strengthen the translational relevance of this murine model.

5. Conclusion

This study demonstrated that chronic scrotal heat stress impairs male sexual performance in a dose- and time-dependent manner. Our novel finding is the characterization of a behavioral tipping point: while moderate heat (37°C) causes a progressive decline, severe heat (40°C) induces a complete collapse of all copulatory behaviors after five weeks, linking physiological damage to total loss of function. This study established a robust murine model with sensitive behavioral endpoints for assessing heat-induced reproductive dysfunction.

Future studies should use this model to investigate the reversibility of these impairments and to identify early biomarkers predictive of functional decline. This study provides an essential platform for screening novel therapeutics aimed at preserving male fertility. Clinically, our findings underscore the reproductive risks associated with occupational heat exposure and rising global temperatures, highlighting the need for protective strategies in both veterinary and human medicine.

Acknowlegments

The authors gratefully acknowledge the partial support provided by Hue University under the Core Research Program, Core Research Group on Regenerative Medicine (NCTB.DHH.2024.02).

6. Declarations

6.1. Ethical considerations

All experimental procedures involving animals were conducted in accordance with the ARRIVE guidelines and approved by the Animal Ethics Committee of Hue University (Certificate No. HUVN0057, dated March 31, 2025). Male ICR mice were maintained under controlled laboratory conditions with free access to food and water and acclimated prior to experimentation. Appropriate measures were taken throughout the study to minimize pain and distress. Surgical procedures for the preparation of stimulus females were performed under general anesthesia and analgesia, followed by postoperative monitoring and supportive care. During the scrotal heat-stress procedure and sexual behavior assessments, animals were handled using standardized protocols, including controlled heat exposure and pre-test habituation in a low-light environment to reduce stress and ensure animal welfare.

6.2. Use of artificial intelligence (AI)

A generative AI tool was used solely to assist with language editing and improving the clarity/structure of the manuscript text (e.g., grammar, wording, and organization). AI was not used for data processing, statistical analysis, figure generation, or interpretation of results. All content was reviewed and approved by the authors, who take full responsibility for the final manuscript.

6.3. Conflict of interest

The authors declare that they have no known competing financial interests or personal relationships that could have influenced the work reported in this paper.

6.4. Funding

Financial support for this research was provided by the Research Projects in Science and Technology program of the Vietnamese Ministry of Education and Training under Grant number B2023-DHH-11.

References

Aldahhan, R. A., & Stanton, P. G. (2021). Heat stress response of somatic cells in the testis. *Molecular and Cellular Endocrinology, 527*, 111216.

Bui-Le, T. N., & Hoang-Tan, Q. (2023). Protective effect of *Curculigo orchioides* Gaertn. extract on heat stress-induced spermatogenesis complications in murine model. *Zhongguo Zhong Yao Za Zhi, 45*(4), 3255–3267.

Cai, H., Qin, D., & Peng, S. (2021). Responses and coping methods of different testicular cell types to heat stress: Overview and perspectives. *Zhonghua Nan Ke Xue, 41*(6), 564–569.

Durairajanayagam, D., Agarwal, A., & Ong, C. (2015). Causes, effects and molecular mechanisms of testicular heat stress. *Reproductive BioMedicine Online, 30*(1), 14–27.

Dutta, S., Majzoub, A., & Agarwal, A. (2019). Oxidative stress and sperm function: A systematic review on evaluation and management. *Arab Journal of Urology, 17*(2), 87–97.

Feige-Diller, J., Krakenberg, V., Bierbaum, L., Seifert, L., Palme, R., Kaiser, S., Sachser, N., & Richter, S. H. (2020). The effects of different feeding routines on welfare in laboratory mice. *Frontiers in Veterinary Science, 6*, 479. https://doi.org/10.3389/fvets.2019.00479

Hafez Hafez, M., El-Sayed El-Kazaz, S., El-Neweshy, M. S., Shukry, M., Ghamry, H. I., & Tohamy, H. G. (2025). Resveratrol mitigates heat stress-induced testicular injury in rats: enhancing male fertility via antioxidant, antiapoptotic, pro-proliferative, and anti-inflammatory mechanisms. *Naunyn-Schmiedeberg's Archives of Pharmacology, 398*(7), 8359–8373. https://doi.org/10.1007/s00210-024-03759-4

Hamilton, T. R. S., Mendes, C. M., Castro, L. S., Assis, P. M., Perez Siqueira, A. F., Delgado, J. C., Goissis, M. D., Muiño-Blanco, T., Cebrián-Pérez, J. Á., Visintin, J. A., & Assumpção, M. E. O. D'A. (2016). Evaluation of lasting effects of heat stress on sperm profile and oxidative status of ram semen and epididymal sperm. *Oxidative Medicine and Cellular Longevity, 2016*, 1687657. https://doi.org/10.1155/2016/1687657

Hansen, P. J. (2009). Effects of heat stress on mammalian reproduction. *Philosophical Transactions of the Royal Society B: Biological Sciences, 364*(1534), 3341–3350.

Hoang-Thi, A. P., Dang-Thi, A. T., Phan-Van, S., Nguyen-Ba, T., Truong-Thi, P. L., Le-Minh, T., Nguyen-Vu, Q. H., & Nguyen-Thanh, T. (2022). The impact of high ambient temperature on human sperm parameters: a meta-analysis. *Iranian Journal of Public Health, 51*(4), 710–723. https://doi.org/10.18502/ijph.v51i4.9232

Houston, B. J., Nixon, B., King, B. V., & Aitken, R. J. (2018). Heat exposure induces oxidative stress and DNA damage in the male germ line. *Biology of Reproduction, 98*(4), 593–606.

Khan, I., & Mesalam, A. (2023). Heat stress as a barrier to successful reproduction and potential alleviation strategies in cattle. *Animals, 13*(14), 2145.

Kim, B., Park, K., & Rhee, K. (2013). Heat stress response of male germ cells. *Cellular and Molecular Life Sciences, 70*(15), 2623–2636.

Lin, P. H., Chen, Y. K., Zhao, J. H., & Wang, Z. (2021). Exertional heat stroke on fertility, erectile function, and testicular morphology in male rats. *Scientific Reports, 11*(1), 3539.

Liu, Z.-W., Wang, L., Wang, Z.-W., & Zhang, X.-X. (2020). Assessment of sexual behavior of male mice. *Journal of Visualized Experiments, 157*, e60154.

Luengo-Mateos, M., Borràs, M., & Esteve-Codina, A. (2024). Protocol for ovariectomy and estradiol replacement in mice. *STAR Protocols, 5*(1), 102910.

Nguyen-Thanh, T., Pham, N. T., Nguyen, T. H., & Bui, H. T. (2022). Chronic scrotal heat stress causes testicular interstitial inflammation and fibrosis: An experimental study in mice. *International Journal of Reproductive Biomedicine, 20*(7), 569–580.

Ogawa, S., Lubahn, D. B., Korach, K. S., & Pfaff, D. W. (2000). Abolition of male sexual behaviors in mice lacking estrogen receptors alpha and beta (αβ ERKO). *Proceedings of the National Academy of Sciences of the United States of America, 97*(26), 14737–14741.

Paul, C., Teng, S., & Saunders, P. T. (2009). A single, mild, transient scrotal heat stress causes hypoxia and oxidative stress in mouse testes, which induces germ cell death. *Biology of Reproduction, 80*(5), 913–919.

Phumsatitpong, C., Wagenmaker, E. R., & Moenter, S. M. (2021). Neuroendocrine interactions of the stress and reproductive axes. *Frontiers in Neuroendocrinology, 63*, 100928.

Plant, T. M. (2015). 60 years of neuroendocrinology: The hypothalamo-pituitary-gonadal axis. *Journal of Endocrinology, 226*(2), T41–T54.

Rhodes, G. J. (2017). Surgical preparation of rats and mice for intravital microscopic imaging of abdominal organs. *Methods, 128*, 129–138.

Robinson, B. R., Netherton, J. K., Ogle, R. A., & Baker, M. A. (2023). Testicular heat stress: A historical perspective and two postulates for why male germ cells are heat sensitive. *Biological Reviews, 98*(2), 603–622. https://doi.org/10.1111/brv.12921

Xiong, Y., Li, J., & He, S. (2022). Zinc protects against heat stress-induced apoptosis via the inhibition of endoplasmic reticulum stress in TM3 Leydig cells. *Biological Trace Element Research, 200*(2), 728–739.

Zhang, M. H., Zhang, X., Wang, M., Li, J., Xu, Y., & Wu, B. (2015). Scrotal heat stress causes sperm chromatin damage and cysteinyl aspartate-specific proteinases 3 changes in fertile men. *Journal of Assisted Reproduction and Genetics, 32*(5), 747–755.

Zhang, P., Zheng, Y., Lv, Y., Li, F., Su, L., Qin, Y., & Zeng, W. (2020). Melatonin protects the mouse testis against heat-induced damage. *Molecular Human Reproduction, 26*(2), 65–79. https://doi.org/10.1093/molehr/gaaa002

Zhao, Z., Cai, Y., Lin, X., Liu, N., Qin, Y., & Wu, Y. (2024). The role of heat-induced stress granules in the blood-testis barrier of mice. *International Journal of Molecular Sciences, 25*(7), 3637.